Food Chemistry 493 (2025) 146015

Contents lists available at ScienceDirect

Food Chemistry

journal homepage: www.elsevier.com/locate/foodchem

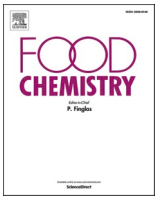

Modification of structural properties and potential allergenicity of ovalbumin induced by ultrasound treatment during *in vitro* digestion

Jing Yang [a,b,*], Nandan Kumar [c], Hong Kuang [a], Yonghui Li [c,**], Jiajia Song [d]

[a] School of Food Science and Engineering, Chongqing Technology and Business University, Chongqing 400067, China
[b] Modern Industry Faculty of Food Nutrition and Health (Hot Pot), Chongqing Technology and Business University, Chongqing 400067, China
[c] Department of Grain Science and Industry, Kansas State University, Manhattan, KS 66506, USA
[d] College of Food Science, Southwest University, Chongqing 400715, China

ARTICLE INFO

Keywords:
Ultrasonication
Egg allergy
Structure property
Molecular dynamics simulation

ABSTRACT

Egg proteins, particularly ovalbumin (OVA), are a major cause of food allergies, especially in children. This study investigated the impact of ultrasound treatment on the molecular structure, digestibility, and allergenicity of OVA. Enzyme-linked immunosorbent assay (ELISA) analysis demonstrated that ultrasound treatment enhanced the enzymatic hydrolysis of OVA during *in vitro* gastrointestinal digestion, significantly reducing its allergenicity. Structural modifications were evaluated using fluorescence spectroscopy, circular dichroism spectroscopy, and molecular dynamics simulations. Following digestion, ultrasound treatment reduced α-helix content by 10 %, increased β-sheet content by 31 %, and enhanced exogenous fluorescence intensity by 33 % compared to undigested OVA. Additionally, ultrasound treatment increased the free sulfhydryl groups and surface hydrophobicity. The binding affinity between ultrasound-treated OVA and trypsin was enhanced, likely due to disruption of OVA's native structure and exposure of cleavage sites. This study demonstrates that ultrasound treatment modifies OVA structure and epitope residues, potentially reducing its allergenicity.

1. Introduction

Food allergies have emerged as a significant global public health issue, with a marked increase in incidence imposing considerable burdens on healthcare systems. Among common food allergens, eggs and milk rank as the primary triggers for young children (Mack et al., 2023). Egg white protein, in particular, is a major allergenic component worldwide, with reported prevalence rates ranging from 1.6 % to 10.1 % (Taniguchi et al., 2022). Currently, the only preventive measure against egg allergies is strict avoidance of egg-containing products-a challenging endeavor given the widespread use of egg-derived ingredients in processed foods (Mack et al., 2023). Consequently, reducing the allergenic potential of egg white proteins has become a critical focus for risk mitigation. Studies indicate that conventional food processing techniques, such as thermal treatment, can partially reduce allergenicity by modifying protein structures. However, these methods often compromise the sensory and nutritional quality of egg whites, adversely affecting product acceptability (Zhu et al., 2018b). Moreover, traditional approaches frequently prove insufficient in completely eliminating allergenicity due to the inherent stability of food allergens against heat and enzymatic degradation (López-Expósito et al., 2008). These limitations have spurred growing interest in innovative non-thermal technologies as potential alternatives.

Ultrasound is a non-thermal processing technology used in food production. Compared to traditional thermal treatments, ultrasound is considered a promising method in the food industry due to its potential to develop green, relatively mild, time-saving, and energy-efficient processes that enhance food quality and safety (Tao & Sun, 2015). During ultrasound processing, cavitation phenomena produce chemical reactions and intense physical forces, including extremely high temperatures, high pressures, shear forces, and shock waves, which collectively mediate substantial conformational rearrangements in protein tertiary structures, thereby modulating their functional properties. It is reported that ultrasound treatment (900 W, 60 min) disrupted and denatured α-casein (α-CN) without change of molecular weight of α-CN (C. Wang et al., 2020). These processed α-CN molecules underwent aggregation to form larger protein complexes with more open conformational arrangements. Notably, ultrasound treatment in this study significantly

* Corresponding author at: Chongqing Technology and Business University, Chongqing 400067, China.
** Corresponding author at: Kansas State University, Manhattan, KS 66506, USA.
E-mail addresses: jyang@ctbu.edu.cn (J. Yang), yonghui@ksu.edu (Y. Li).

https://doi.org/10.1016/j.foodchem.2025.146015
Received 17 April 2025; Received in revised form 26 July 2025; Accepted 18 August 2025
Available online 20 August 2025

reduced both the Immunoglobulin (Ig) E -binding capacity of α-CN and subsequent mast cell degranulation responses. The tertiary structure and emulsifying activity of ovalbumin (OVA) was changed by the ultrasound treatment (Xiong et al., 2016). However, high-intensity ultrasonication (600–800 W) paradoxically increased OVA's allergenicity, as evidenced by enhanced IgG/IgE recognition (W. H. Yang et al., 2017). Consequently, adjustment of ultrasound treatment conditions is required to effectively induce structural alterations and attenuate OVA's allergenicity.

Digestive stability represents a fundamental characteristic shared by most food allergens, enabling their survival through the gastrointestinal tract and subsequent interaction with the immune system. The allergenicity of proteins after being digested in the gastrointestinal tract depends on the stability of the proteins against enzymatic hydrolysis during the digestive process. The severity of food allergic reactions depends on the intact passage of allergenic proteins through the gastrointestinal tract while preserving sufficient IgE-binding epitopes to trigger mast cell activation (Bu et al., 2013). *In vitro* digestion is a digestion simulation method based on mimicking the stomach and intestinal digestive processes, with advantages such as simplicity, speed, low cost, and high reproducibility (Brodkorb et al., 2019). OVA demonstrated high pepsin resistance with retained IgE reactivity during gastric digestion, but showed significantly reduced allergenicity following duodenal proteolysis when tested against allergic patients' sera (Martos et al., 2010). *In vitro* simulation results show that traditional thermal processing is unfavorable for the digestive degradation of OVA, while novel non-thermal technologies (ultrasound, high-pressure processing, irradiation) induce favorable conformational changes in food proteins that simultaneously: (i) enhance gastrointestinal digestibility and (ii) reduce potential allergenicity. However, residual IgE reactivity persists in egg white proteins even after combined enzymatic hydrolysis and simulated digestion, suggesting partial retention of immunodominant epitopes (Behzad Gazme et al., 2020). Microwave pretreatment assisting enzymolysis further increases in the hydrolysis of OVA and decreases the allergenicity of OVA (Liu et al., 2023). Ultrasound treatment accelerates enzymatic hydrolysis of rice protein and rapeseed protein (Jian Jin et al., 2016; S. Li et al., 2016). Emerging evidence indicates that ultrasonic processing induces structural modifications in OVA, leading to altered IgE-binding capacity and reduced allergenic potential (W. H. Yang et al., 2017), but ultrasound-accelerated enzymatic hydrolysis of OVA and its allergenicity changes during gastrointestinal digestion remain unclear.

It is hypothesized that ultrasound treatment induces conformational modifications in OVA that enhance its susceptibility to enzymatic hydrolysis and attenuate its IgE-binding capacity during simulated gastrointestinal digestion, thereby mitigating its allergenic potential. To evaluate this hypothesis, the present study systematically investigated the structural alterations and allergenicity of ultrasound-treated OVA under simulated gastrointestinal digestion. Structural changes in OVA were characterized using circular dichroism (CD) spectroscopy, intrinsic fluorescence spectroscopy, and sodium dodecyl sulfate–polyacrylamide gel electrophoresis (SDS-PAGE). The IgE-binding capacity of OVA was quantitatively assessed *via* enzyme-linked immunosorbent assay (ELISA). Furthermore, molecular dynamics (MD) simulations were employed to elucidate the molecular basis of the observed changes in digestive stability. Collectively, these analyses provide mechanistic insights into the reduction of OVA allergenicity induced by ultrasound treatment and contribute to a deeper understanding of the structure–immunoreactivity relationship in food allergens.

2. Materials and methods

2.1. Reagents and materials

Ovalbumin (OVA; ≥98 % purity, catalog no. A5503) and 1-anilinonaphthalene-8-sulfonate (ANS; A1028) were procured from Sigma-Aldrich (St. Louis, MO, USA). Immunological reagents including goat anti-mouse IgE secondary antibody (SA5–10262) and horseradish peroxidase (HRP)-conjugated antibody (SA5–10263) were sourced from Thermo Fisher Scientific (Cleveland, OH, USA), and purified mouse anti-OVA IgE (MCA225, clone 2C6) were procured from Bio-Rad Laboratories (Hercules, CA, USA). Digestive enzymes (pepsin [P8160] and trypsin [T8150]) were obtained from Solarbio (Beijing, China). Electrophoresis reagents, SDS-PAGE sample loading buffer (2×; P0015B), Coomassie Brilliant Blue R-250 (P0017B), tetramethylbenzidine (TMB; P0215), and protein molecular weight marker (P0060S), were purchased from Beyotime Biotechnology (Shanghai, China). All other chemicals used were of analytical grade purity.

2.2. Ultrasonic treatments

OVA was dissolved in distilled water (1 mg/mL) and placed in an ultrasonic device Scientz-IID (25 kHz and 100 W, NingBo Scientz Biotechnology Co., Ltd., Ningbo, Zhejiang, China) with processing times of 0, 20, 40, and 60 min (working for 3 s, resting for 7 s). Temperature was maintained at 15–20 °C throughout the ultrasonication process. After ultrasonic treatment, samples were store at −80 °C followed by freeze-drying for further analysis.

2.3. In vitro digestion

A two-stage digestion was performed following established methods (Abraham et al., 2015). For gastric phase, OVA solution (100 mg/mL) was mixed 1:1 with 1.25× simulated gastric fluid (SGF, pH 3.0 ± 0.1), containing 600 U/mL pepsin and 0.075 mmol/L $CaCl_2$, then incubated (37 °C, 200 rpm, 2 h). The reaction was terminated by pH adjustment to 7.0. For intestinal phase, gastric digesta was mixed 1:1 with 1.25× simulated intestinal fluid (SIF, pH 7.0 ± 0.1) containing 100 U/mL trypsin, 10 mmol/L bile salts, and 0.3 mmol/L $CaCl_2$, followed by incubation (37 °C, 200 rpm, 2 h). Samples were heat-inactivated (95 °C, 5 min) and stored at −80 °C.

2.4. Analysis of IgE-binding ability

The IgE reactivity of native and ultrasound-treated OVA was determined using an indirect ELISA protocol adapted from our previous study (J. Yang et al., 2024). Protein samples (100 μL/well at 1 mg/mL in 50 mM carbonate buffer, pH 9.6) were coated onto 96-well plates overnight at 4 °C. After blocking with 5 % skim milk in PBST (37 °C, 1 h), plates were incubated with either: (i) pooled sera from OVA-sensitized mice (1:100 dilution) prepared in our previous study (J. Yang et al., 2024) or (ii) commercially anti-OVA monoclonal antibody (1:1000 dilution). Following incubation (37 °C, 1 h) and washing, bound IgE was detected using HRP-conjugated secondary antibody (1:2000, 37 °C, 30 min). The reaction was developed with TMB substrate (15 min, 37 °C), stopped with 2 M H_2SO_4, and absorbance measured at 450 nm using a Tecan Infinite M200 Pro microplate reader (Tecan, Männedorf, Switzerland). All samples were analyzed in triplicate, with results expressed as percentage reactivity relative to untreated OVA controls.

2.5. SDS-PAGE analysis of OVA molecular weight distribution

The molecular weight profiles of native and processed OVA were characterized by SDS-PAGE according to our established protocol (J. Yang et al., 2024). Briefly, protein samples (1 mg/mL) were denatured in 2× loading buffer (1:1 *v*/v) at 95 °C for 10 min. Electrophoresis was conducted using a discontinuous gel system (5 % stacking and 12 % separating gels) at constant voltage (120 V). Gels were visualized by silver staining for enhanced sensitivity.

2.6. Determination of degree of hydrolysis

The proteolytic degradation of OVA was quantified using the o-phthaldialdehyde (OPA) method (Li Li et al., 2019). Briefly, 400 μL of each sample was mixed with 3 mL of freshly prepared OPA reagent and incubated for 2 min at room temperature. Absorbance was immediately measured at 340 nm using a spectrophotometer, with L-serine standard solution and ultrapure water serving as the standard curve and blank control, respectively.

2.7. Circular dichroism (CD) analysis

The secondary structure changes of ultrasound-treated OVA were analyzed by CD spectroscopy using a Chirascan spectropolarimeter (Applied Photophysics, Leatherhead, Surrey, UK). Protein samples were prepared at 0.2 mg/mL and measured in a 1 mm pathlength quartz cuvette. CD spectra were recorded from 190 to 240 nm at 25 °C with a bandwidth of 1.0 nm and scan rate of 100 nm/min, accumulating three scans per sample for improved signal-to-noise ratio. After baseline correction with buffer-only spectra, the raw ellipticity data (in millidegrees, mdeg) were analyzed using CDNN deconvolution software (Version 2.1) to quantify the relative percentages of secondary structure elements, including α-helix, β-sheet, β-turn, and random coil conformations. All measurements were performed in triplicate following our established protocol (J. Yang et al., 2024).

2.8. Intrinsic fluorescence spectrum analysis

The tertiary structural changes of OVA were characterized by intrinsic fluorescence spectroscopy using an F-7000 spectrofluorometer (Hitachi, Tokyo, Japan). Protein samples (0.1 mg/mL) were excited at 280 nm (selective for tryptophan residues), with emission spectra recorded from 310 to 400 nm using 5 nm slit widths for both excitation and emission. Spectra were acquired at a scan rate of 1200 nm/min with photomultiplier tube voltage set to 400 V, collecting three independent scans per sample for reproducibility. All measurements were conducted at 25 °C following our standardized protocol (J. Yang et al., 2024).

2.9. Exogenous fluorescence spectrum analysis

The surface hydrophobicity of ultrasound-treated OVA was evaluated using ANS binding assays. Protein samples (0.1 mg/mL) were mixed with ANS solution (4 mmol/L in PBS) at a 1:50 (*v*/v) ratio and incubated in the dark for 15 min at 25 °C. Fluorescence spectra were acquired using an F-7000 spectrofluorometer (Hitachi, Tokyo, Japan) with the following parameters: excitation at 390 nm, emission scanning from 440 to 600 nm, excitation/emission slit widths of 10 nm, photomultiplier tube voltage of 400 V, and a scan speed of 1200 nm/min. Three consecutive scans were averaged for each sample, with PBS-ANS blanks subtracted to correct background signals (J. Yang et al., 2024).

2.10. Free sulfhydryl (SH) analysis

The free SH content of OVA was determined using Ellman's assay with modifications. Protein samples (1 mg/mL in Tris-glycine buffer: 86 mM Tris, 4 mM EDTA-Na, 90 mM glycine, pH 8.0) were reacted with 5,5′-dithiobis (2-nitrobenzoic acid) (DTNB, 4 mg/mL in the same buffer) at a 1:100 (v/v) ratio. After 1 h incubation in the dark at 25 °C, absorbance was measured at 412 nm using a UV-1102 spectrophotometer (Tianmei Techcomp, Shanghai, China). Free SH content was calculated as: SH (μ mol/g) = $73.53 \times A_{412}/C$, where A_{412} is the absorbance of the sample at 412 nm and C represents the sample concentration (Li Li et al., 2019).

2.11. Surface hydrophobicity

The surface hydrophobicity of OVA was quantified using ANS as a fluorescent probe according to established methods (Li et al., 2022a; J. Yang et al., 2024). Protein samples were serially diluted in phosphate-buffered saline (PBS, pH 7.4) to concentrations of 0.05–0.25 mg/mL (0.05, 0.1, 0.15, 0.2, and 0.25 mg/mL). For each measurement, 20 μL of 8 mM ANS solution (in PBS) was added to 4 mL of protein solution (final ANS concentration: 40 μM) and vortexed thoroughly. After 15 min incubation in the dark at 25 °C, fluorescence intensity was measured using a spectrofluorometer with an excitation wavelength of 390 nm and an emission wavelength of 470 nm.

2.12. Molecular dynamics simulation

MD simulations were conducted with GROMACS version 2023.3 (Abraham et al., 2015), using the CHARMM27 force field. The structures of OVA, OVA-pepsin, and OVA-trypsin complexes were taken from our previous study (J. Yang et al., 2024; J. Yang et al., 2025), where they were validated for stability through extensive MD simulations. The protein was solvated in a dodecahedron box filled with TIP3P water molecules, and the system was neutralized by adding counter ions depending on the charge of the system. Energy minimization was carried out using the steepest descent algorithm for 50,000 steps to ensure proper relaxation. The system was equilibrated in two stages: first, in the NVT ensemble using a V-rescale thermostat for 100 ps, and second, in the NPT ensemble using the Parrinello-Rahman barostat for 100 ps. Production MD simulations were conducted for a total duration of 100 ns with a time step of 2 fs, using the leap-frog integrator for numerical integration of the equations of motion. Long-range electrostatic interactions were calculated using the Particle Mesh Ewald (PME) method, and the bond lengths involving hydrogen atoms were constrained using the LINCS algorithm.

In this study, we employed pressure variations generated by positive and negative square waves (Fig. S1) to simulate ultrasonic conditions, adopted from literature (Gao et al., 2024; Han et al., 2022). These pressure variations alternated between high (+50 MPa) and low (−50 MPa) phases, mimicking the compression and rarefaction effects of ultrasound. Each cycle lasted 2.5 ns, corresponding to an ultrasound frequency of 400 MHz. Over the 100 ns simulation time, this approach ensures that the protein is exposed to sustained mechanical stress, replicating the continuous mechanical forces induced by ultrasound waves. These conditions were chosen to mimic the mechanical stress experienced by proteins during ultrasonic treatment. While the experimental study employed ultrasonic treatment at 100 W, which likely corresponds to higher pressure, the inclusion of 50 MPa allows to investigate the effects of ultrasonic pressure and its potential role in inducing structural changes. It is important to note that MD simulations operate on a nanosecond (ns) timescale, which is significantly shorter than the experimental treatment times (minutes). Directly mimicking the 25 kHz ultrasound frequency (with a pressure switch time of 20 μs) in MD simulations is computationally impractical due to the enormous number of steps required. Therefore, the simulation conditions (400 MHz, 50 MPa) were selected to replicate the mechanical effects of ultrasound within a computationally feasible timescale. While these conditions are not directly comparable to the experimental treatment times, they provide molecular-level insights into the structural and conformational changes induced by ultrasound, which align with and complement the experimental findings.

MD simulations were conducted for four systems including native OVA (OVA_Control), ultrasound-treated OVA without digestion (OVA_US), ultrasound-treated OVA after digestion with pepsin (OVA_US_Pepsin), and ultrasound-treated OVA after digestion with trypsin (OVA_US_Trypsin). Output trajectories were saved every 10 ps for analysis. These simulations provide insights into the structural and conformational changes induced by ultrasound, as well as the

interactions within the OVA-pepsin and OVA-trypsin complexes. PDBePISA was utilized to analyze the interaction areas and binding energies of protein complexes under ultrasonic treatment, while LigPlot was employed to visualize and characterize the hydrogen bonds and hydrophobic interactions at the binding interfaces (Laskowski et al., 2018; Wallace et al., 1995).

2.13. Statistical analysis

All experimental data were analyzed using SPSS Statistics 23 (IBM Inc., Chicago, IL, USA) with one-way analysis of variance (ANOVA) followed by Duncan's multiple range test for post-hoc comparisons. Statistical significance was established at $p < 0.05$. Data are presented as mean ± standard error of the mean (SEM) of at least three independent replicates. Graphical representations were generated and refined using GraphPad Prism 9 (GraphPad Software Inc., San Diego, CA, USA), with consistent formatting applied to all figs.

3. Results

3.1. Effects of ultrasound on the hydrolysis of OVA

We firstly investigated the impact of ultrasound on the hydrolysis of OVA. As shown in Fig. 1A, the degree of hydrolysis of untreated-OVA increased to 8.37 ± 0.17 % after gastrointestinal digestion, which was further increased by ultrasound treatment, and reached 9.67 ± 0.15 % after 60 min of ultrasound treatment. In addition, SDS-PAGE analysis was conducted to elucidate the influence of ultrasound and digestion treatment on the molecular weight of OVA. As shown in Fig. 1B, the molecular weight of native OVA is 45 kDa, and after *in vitro* digestion, the 45 kDa band intensity weakened, and new bands around 10–15 kDa appeared, compared to the undigested OVA. All these findings suggest that ultrasound induced hydrolysis of OVA and produced small molecular proteins during digestion.

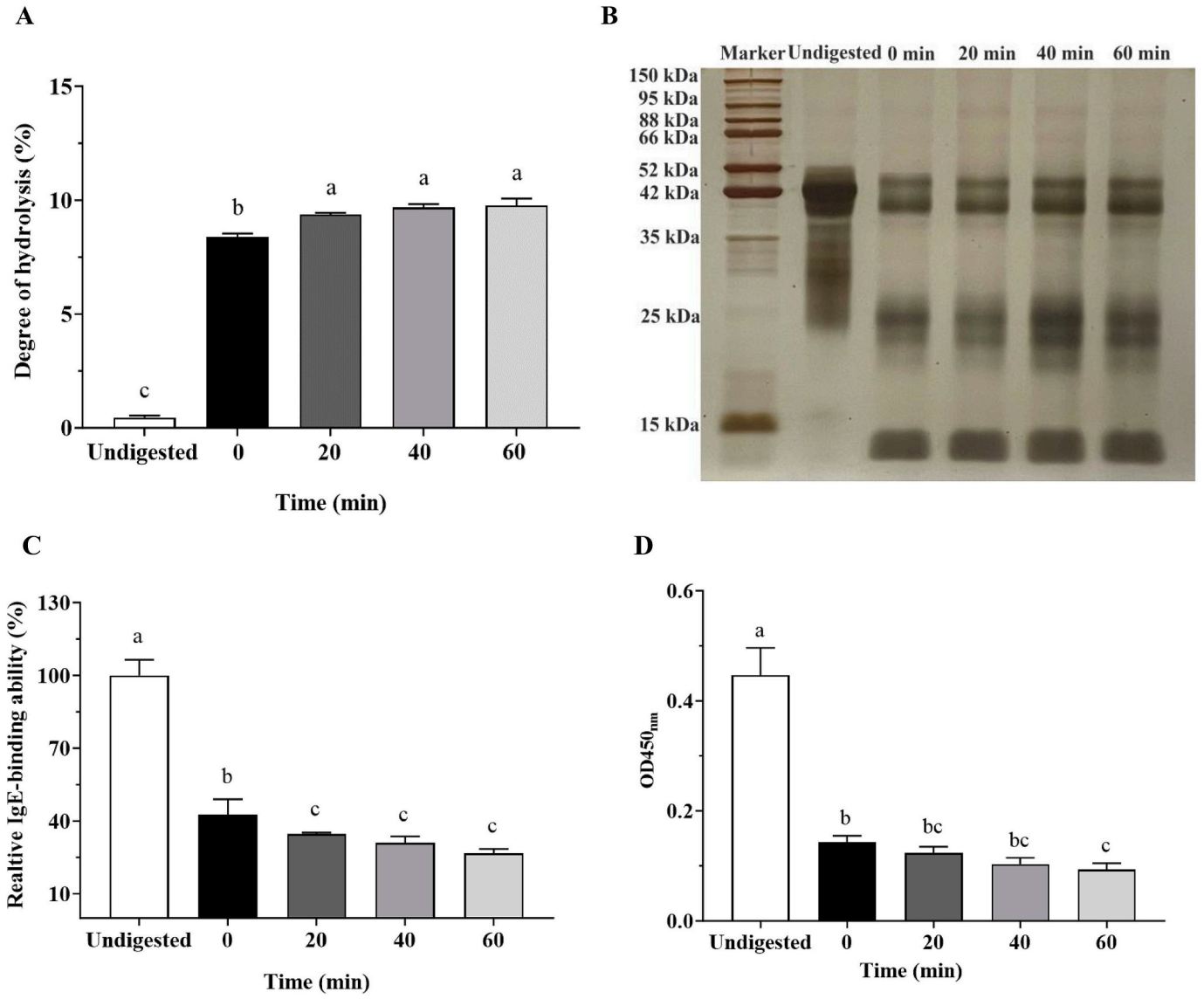

Fig. 1. Changes in hydrolysis and IgE-binding capacity of ultrasound-treated OVA. OVA was treated with ultrasound for 20, 40, and 60 mins, the degree of hydrolysis of ultrasound-treated OVA after *in vitro* digestion (A); *in vitro* digestion products of ultrasound-treated OVA were separated by SDS-PAGE and visualized with silver staining (B); IgE-binding ability of ultrasound-treated OVA after *in vitro* digestion were analyzed using polyclonal antibody in mouse serum (C) and commercial monoclonal antibody (D). The undigested sample is OVA without ultrasound and digestion treatment. Data are presented as the mean ± standard error of the mean (SEM), $n = 3$. Different superscript letters in the fig. A, C, D indicate significant differences ($p < 0.05$).

3.2. Effects of ultrasound on the IgE-binding capacity of OVA

The polyclonal OVA-IgE antibody from mouse serum prepared in the lab and monoclonal OVA-IgE antibody purchased from Biorad to investigate the effect of ultrasound on the IgE binding capacity of OVA using the indirect ELISA (iELISA) method. Results from the mouse serum polyclonal IgE antibody experiment (Fig. 1C) showed that the IgE binding capacity significantly decreased by 57.35 % after *in vitro* digestion, compared with the undigested OVA. This indicates that digestive enzymes can destroy some allergenic epitopes of OVA, especially linear epitopes, preventing recognition by IgE receptors. Compared to no-ultrasound-treated OVA (*i.e.*, 0 min), there was significantly reduce in IgE binding capacity of OVA by ultrasound treatment during *in vitro* digestion. Similar results were obtained in the monoclonal

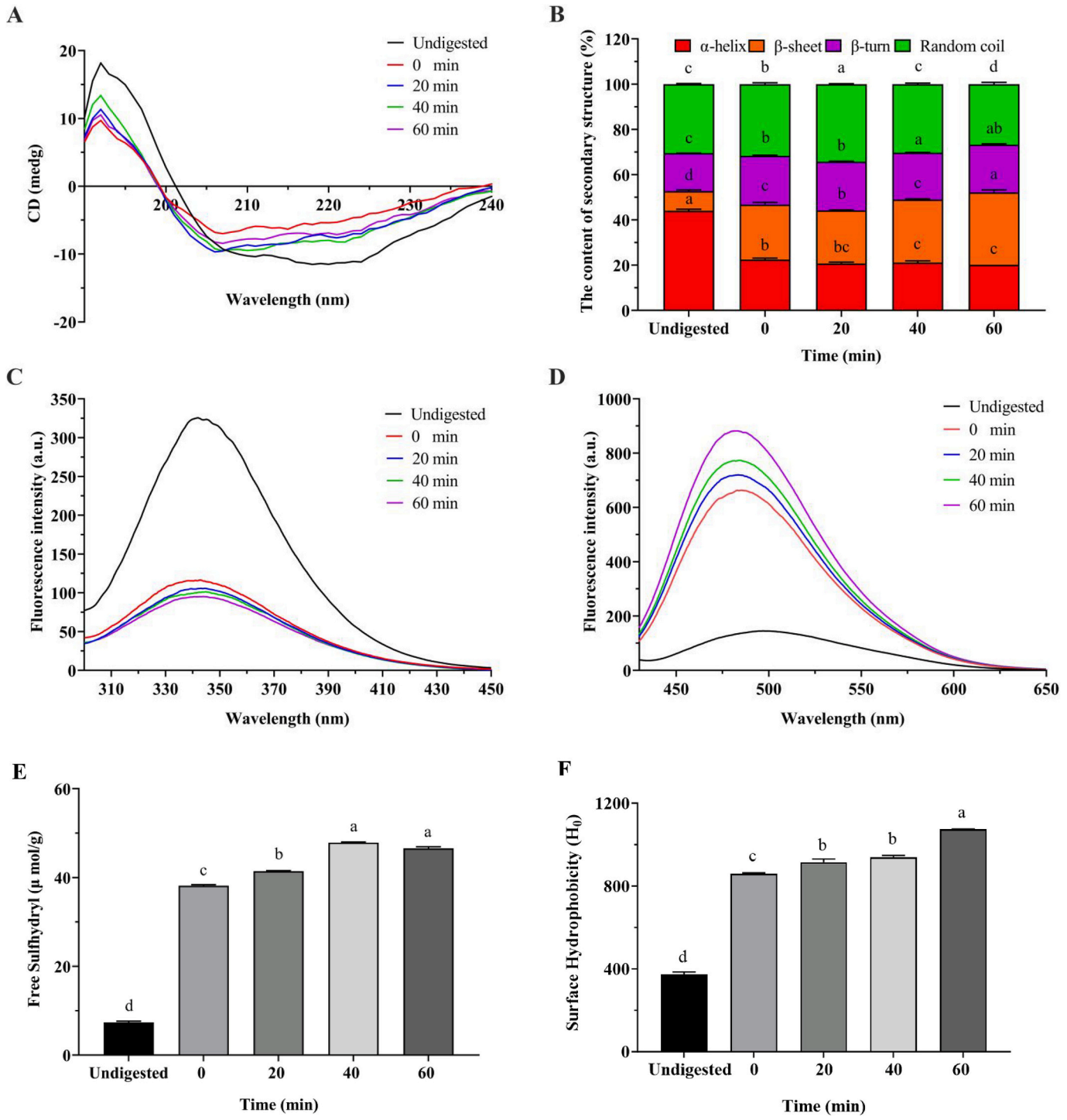

Fig. 2. Changes in the structure and physical properties of ultrasound-treated OVA. OVA was treated with ultrasound for 20, 40, and 60 mins. Structural changes including circular dichroism spectrograms (A), secondary structure changes (B), Intrinsic fluorescence spectroscopy (C) and exogenous fluorescence spectroscopy (D) of ultrasound-treated OVA after *in vitro* digestion. Changes in the content of free surface sulfhydryl groups (E) and surface hydrophobicity (F) of ultrasound-treated OVA after *in vitro* digestion. Data are presented as the mean ± standard error of the mean (SEM), n = 3. Different superscript letters in the fig. B, E, F indicate significant differences ($p < 0.05$).

IgE antibody experiment (Fig. 1D). All these findings suggest that ultrasound treatment has the potential to reduce the allergenicity of OVA.

3.3. Effects of ultrasound on the molecular structure of OVA

CD spectroscopy is an important tool for studying changes in protein secondary structure. The changes in the CD spectra of OVA after ultrasound treatment are shown in Fig. 2A. Compared to the undigested OVA group, the digestion process reduced the α-helix content significantly, and ultrasound treatment led to a further decrease in α-helix content with increasing ultrasound time, with the increased content of β-sheet structure. Compared to the digested OVA without ultrasound treatment, the α-helix content (60 min group) significantly decreased by 10 % and after *in vitro* simulated digestion, while the β-sheet content increased by 31 % (Fig. 2B).

Intrinsic fluorescence spectroscopy analyzes tryptophan/tyrosine fluorescence to evaluate protein tertiary structure changes. This technique detects conformational alterations through shifts in fluorescence emission caused by microenvironmental polarity changes around these aromatic residues (Li et al., 2022b). After digestion, the intrinsic fluorescence intensity of OVA significantly decreased, which was further reduced by ultrasound treatments. At 60 min of ultrasound treatment, the fluorescence intensity decreases to 86.33 ± 2.09 a.u. (Fig. 2C). Hydrophobic interactions are critical for maintaining protein structure, and ANS fluorescence spectroscopy serves as a sensitive tool to probe surface hydrophobicity (Zhou et al., 2016). Compared to undigested OVA, the exogenous fluorescence intensity of OVA increased after digestion and ultrasound treatment. At 60 min of ultrasound treatment, the

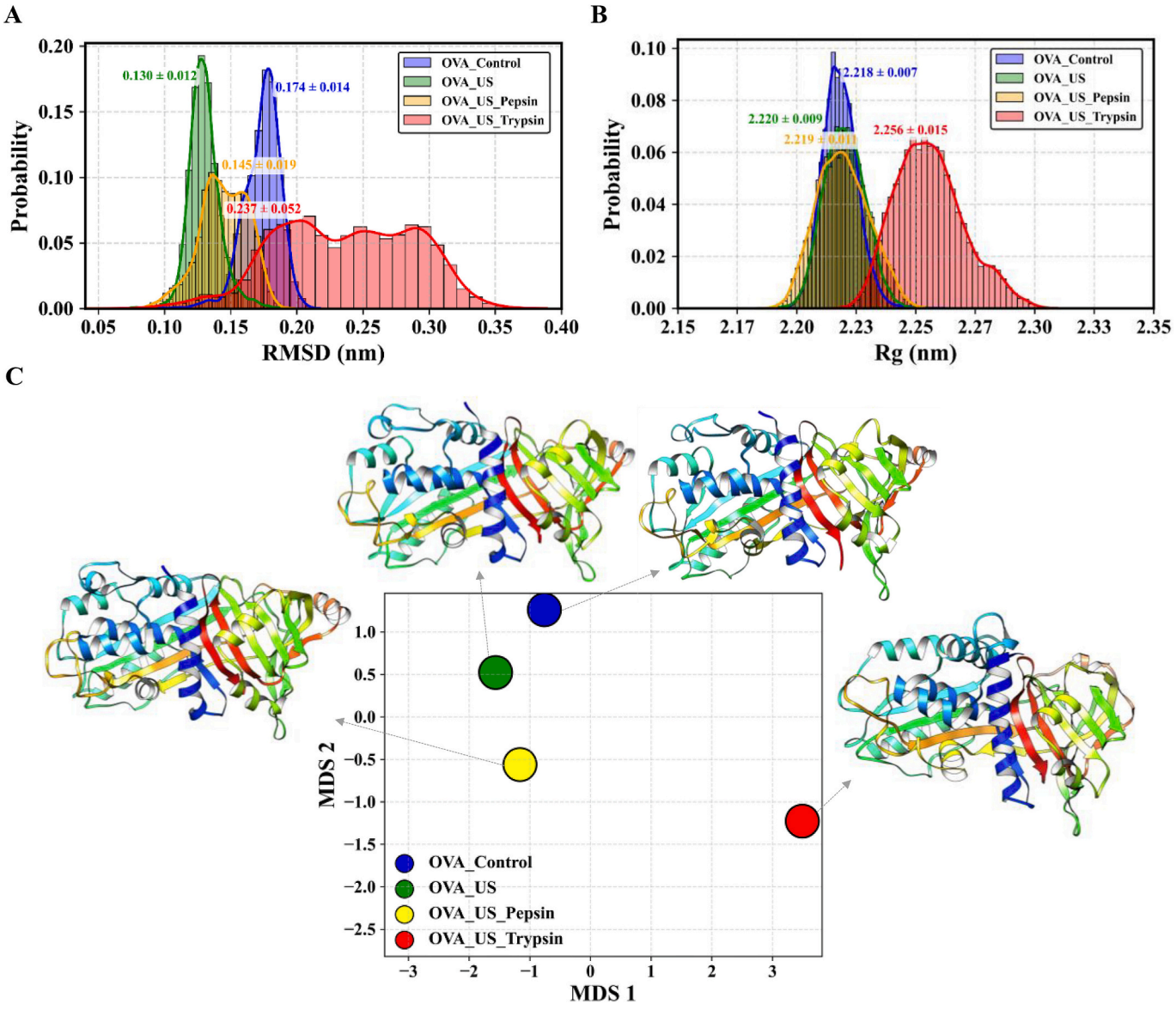

Fig. 3. Structural changes of ultrasound-treated OVA based on Root Mean Square Deviation (RMSD) calculations. (A) Probability distribution of RMSD and (B) radius of gyration (Rg) values (in nm) for untreated control OVA (blue), ultrasound-treated OVA (green), and ultrasound-treated OVA subjected to enzymatic digestion with pepsin (yellow) or trypsin (red). (C) Multi-Dimensional Scaling (MDS) plot illustrating the structural similarity among OVA protein samples based on RMSD calculations. Each circular dot represents an OVA structure, with distinct colors indicating treatment conditions: untreated OVA control (blue), ultrasound-treated OVA (green), ultrasound-treated OVA with pepsin digestion (yellow), and ultrasound-treated OVA with trypsin digestion (red). The respective 3D structures of OVA are displayed alongside the dots, providing a visual representation of conformational changes. The axes (MDS 1 and MDS 2) represent the reduced dimensions derived from the RMSD matrix, highlighting the relative structural differences among the samples. (For interpretation of the references to colour in this figure legend, the reader is referred to the web version of this article.)

fluorescence intensity reached its maximum peak, which is 33 % increase compared with that of the untreated group (Fig. 2D). All the changes in the fluorescence spectrum indicate that ultrasound and digestion treatments alter the tertiary structure of OVA, causing the protein structure to unfold.

3.4. Effects of ultrasound on the physical properties of OVA

The concentration of free sulfhydryl groups exhibits an inverse relationship with disulfide bond formation, representing the dynamic equilibrium between -SH oxidation and S—S reduction. As shown if Fig. 2E-F, the free sulfhydryl content and surface hydrophobicity were increased by digestion process and further enhanced by ultrasound treatment. After 60 min of ultrasound treatment, the free sulfhydryl content increased by 21.05 % compared to OVA without ultrasound treatment ($p < 0.05$). Furthermore, the surface hydrophobicity significantly increased to 1073.33 ± 13.09 (60 min), compared the 0 min group (858.53 ± 7.41). This indicates that ultrasound and digestion disrupted intramolecular disulfide bonds in proteins, exposing hydrophobic groups and free sulfhydryl as the protein molecules unfolded.

3.5. Effect of ultrasound on global structural changes of OVA

To assess the structural stability of OVA under ultrasound treatment, we analyzed the Root Mean Square Deviation (RMSD) of its atomic positions using MD simulations. The results revealed distinct conformational behaviors among the OVA samples, as shown in Fig. 3A. The untreated OVA control exhibited the RMSD values with a peak probability of around 0.174 nm, suggesting a more dynamic conformation. In contrast, ultrasound-treated OVA showed a slightly better stability in the RMSD distribution with a peak probability of around 0.130 nm, indicating that sonication may induce a more compact or rigid structural arrangement. Further enzymatic digestion of ultrasound-treated OVA with pepsin and trypsin resulted in progressively broader RMSD distributions, with peak probabilities around 0.145 nm and 0.237 nm, respectively. After pepsin digestion, the protein retained moderate stability, suggesting partial resistance to proteolytic cleavage. However, ultrasound-treated OVA subjected to trypsin digestion displayed the highest RMSD values, reaching up to 0.237 nm, indicating significant conformational changes and increased flexibility due to the combined effects of ultrasound and enzymatic hydrolysis.

The Radius of Gyration (Rg) analysis (Fig. 3B) provided additional insights into the compactness and overall folding of the protein. The untreated OVA control had the Rg value of 2.218 ± 0.007 nm, consistent with a natively compact and well-folded structure. Ultrasound treatment resulted in a negligible change in Rg (2.220 ± 0.009 nm), suggesting that ultrasound alone did not significantly alter the overall folding of OVA. However, enzymatic digestion following ultrasound treatment led to divergent effects on protein stability. The ultrasonication-treated OVA with pepsin and with trypsin digestion exhibiting Rg values of 2.219 ± 0.007 nm and 2.256 ± 0.015 nm, respectively. Pepsin-digested OVA maintained near-native compactness, aligning with its moderate changes in RMSD and suggesting partial proteolytic resistance. The higher Rg for ultrasonication-treated OVA with trypsin digestion indicates a more extended conformation, likely due to partial unfolding or loosening of the protein structure caused by trypsin digestion. These results suggest that ultrasonication alone stabilizes OVA, while enzymatic digestion progressively changes its structure, with trypsin having the most pronounced effect. This change is consistent with the broader structural flexibility and increased solvent exposure observed in ultrasonication-treated OVA with trypsin digestion, suggesting the synergistic impact of ultrasound and enzymatic treatments on conformational dynamics of OVA protein.

To further assess the structural changes of ultrasound treated-OVA during digestion, Multi-Dimensional Scaling (MDS) analysis was performed based on the RMSD matrix (Fig. 3C). The MDS plot effectively represents the structural relationships among these samples in a 2D space, where the spatial separation of points reflects the structural deviations. The untreated OVA control, ultrasound-treated OVA and ultrasonication-treated OVA with pepsin digestion clustered tightly, indicating minimal structural variation. Notably, ultrasonication-treated OVA with trypsin digestion displayed the most significant separation along both MDS1 and MDS2, confirming the substantial structural changes and increased flexibility observed in the RMSD and Rg analyses. This clear separation in the MDS plot underscores the pronounced impact of trypsin digestion on the structure of OVA following ultrasound treatment. These visualizations highlight the extent of structural disruption induced by the combined effects of ultrasound and trypsin digestion, providing better molecular-level understanding of how these treatments alter OVA structural integrity.

3.6. Effect of ultrasound on residue-wise structural deviations and key residues of OVA

The Root Mean Square Fluctuation (RMSF) analysis provided further insights into the local flexibility and residue-wise conformational changes in OVA under different treatment conditions, as shown in Fig. 4A. The untreated OVA control exhibited relatively low RMSF values across most residues, indicating minimal local fluctuations and a stable structure. Ultrasound-treated OVA showed slightly increased RMSF values, particularly in loop regions and terminal residues, suggesting that ultrasound treatment induces localized flexibility without significantly disrupting the core structure. Enzymatic digestion of ultrasound-treated OVA with pepsin resulted in moderate increases in RMSF values, indicating additional flexibility in specific regions. In contrast, ultrasound-treated OVA subjected to trypsin digestion exhibited the highest RMSF values across multiple residues, particularly in regions such as Lys62-Val80, Tyr112-Pro116, Ala138-Arg143, and Arg340-Arg360. These regions are rich in lysine and arginine, which are primary cleavage sites for trypsin. These findings suggest that trypsin digestion, following ultrasound treatment, leads to significant local unfolding and increased flexibility in OVA, consistent with the broader RMSD distribution and higher Rg values observed for ultrasonication-treated OVA with trypsin digestion.

To further evaluate the structural differences between untreated OVA control and ultrasound-treated OVA with trypsin digestion, a residue-wise RMSD analysis was performed after structural superimposition (Fig. 4B). The RMSD values for each residue were calculated based on C-alpha atom positions, allowing for a detailed assessment of local conformational changes induced by trypsin treatment. The residue-wise RMSD plot demonstrates that most residues exhibit minimal structural deviations, with RMSD values generally remaining below 5.0 Å. However, several residues exceeded this threshold, indicating significant conformational changes in specific regions of the protein. Notably, residues Ser69-Val80 and Val342-Ala353 show peaks exceeding 10 Å, with the most significant deviations observed around residues Glu71-Gly75, reaching an RMSD of approximately 20 Å. These peaks suggest pronounced structural flexibility or possible unfolding in these regions, contributing to the overall structural flexibility observed in ultrasound-treated OVA subjected to trypsin digestion. In addition, a few other residues also showed noticeable RMSD values, including Asn95-Val97, Tyr112-Glu117, Ser237-Gly238, Ser271-Val273, and Ser310-Glu320, further highlighting localized structural changes.

The superimposed 3D structures of untreated OVA control and ultrasound-treated OVA with trypsin digestion (Fig. 4C) further emphasize these major conformational differences and the changes in secondary structure. The structural superimpositions support these observations, showing notable deviations in loop regions and flexible regions. For instance, region Lys62-Asn79 undergoes substantial rearrangement, contributing to the peak observed in the RMSD plot. Similarly, a helical region exhibits marked structural alterations, possibly indicating partial unwinding or reorganization. Changes in

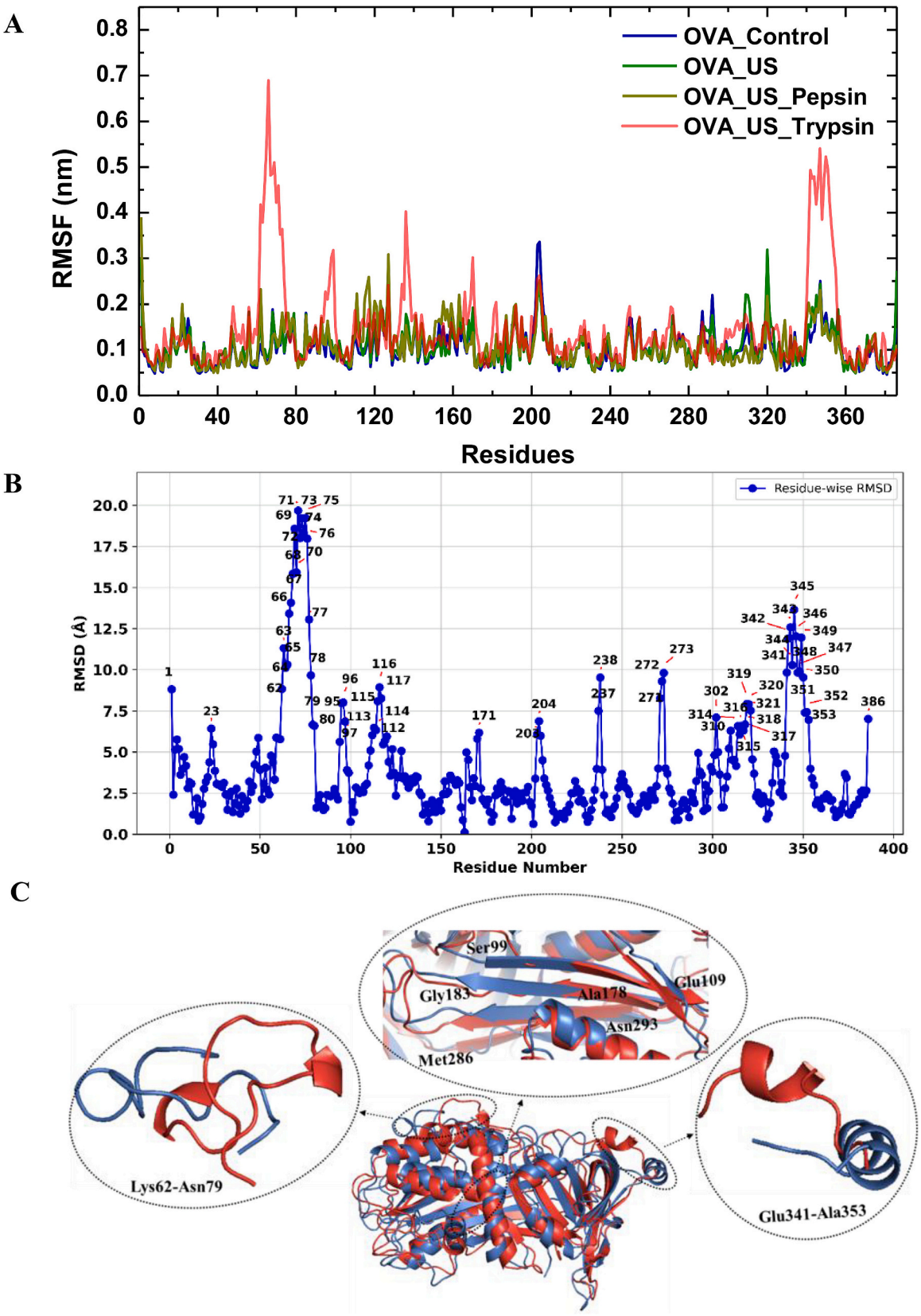

Fig. 4. Residue changes in OVA after *in vitro* digestion. (A-B) The Root Mean Square Fluctuation (RMSF) values (in nm) and Residue-wise Root Mean Square Deviation (RMSD in Å) comparison between untreated OVA control and ultrasound-treated OVA with pepsin and trypsin digestion after structural superimposition. RMSD values (in Å) were calculated based on C-alpha atom positions for each residue. (C) Superimposed 3D structures of untreated OVA control (blue) and ultrasound-treated OVA with trypsin digestion (red), with regions exhibiting significant structural and conformational differences highlighted and zoomed in for detailed visualization. (For interpretation of the references to colour in this figure legend, the reader is referred to the web version of this article.)

Ser99-Glu109, Ala178-Gly183, and Met286-Asn293 demonstrate localized changes in β-sheets, with a deviation in backbone positioning. These findings indicate that specific regions of the protein undergo significant conformational changes, consistent with the increased flexibility and partial unfolding observed in the RMSD, Rg, and RMSF analyses.

3.7. Effect of ultrasound on interaction of the OVA with pepsin and trypsin

The protein-protein interaction analysis provides critical insights into the binding interactions between OVA and the enzymes pepsin and trypsin under different treatment conditions. The hydrogen bond (h-bond) analysis over the 100 ns duration revealed that the native OVA-Pepsin and OVA-Trypsin complexes had seven to nine hydrogen bonds in their native states, *i.e.*, at 0 ns (Fig. 5A). However, the number of h-bond decreased between OVA and pepsin upon ultrasound treatment, reaching one to two hydrogen bonds at 100 ns, suggesting that ultrasound treatment weakens the interactions between OVA and pepsin. In contrast, the ultrasound-treated OVA-Trypsin complex exhibited a substantial increase in hydrogen bonds, reaching ten to eleven hydrogen bonds over 100 ns, indicating enhanced interactions between OVA and trypsin under ultrasound treatment.

To further evaluate the binding energy and interface details, PISA interface analysis was performed (Table 1). The analysis revealed significant differences in the interface area (Å^2), binding free energy (ΔiG, kcal/mol), and *P*-values for the complexes. For the native OVA-Pepsin complex, the interface area was 998.4 Å^2, with a binding free energy of −0.9 kcal/mol, indicating a relatively weak interaction. In contrast, the native OVA-Trypsin complex exhibited a smaller interface area (773.3 Å^2) but a more favorable binding free energy (−3.8 kcal/mol), suggesting a stronger interaction compared to the OVA-Pepsin complex. The native structures of OVA-Pepsin and OVA-Trypsin were taken from our previous study (J. Yang et al., 2025). Following ultrasound treatment, the OVA-Pepsin complex showed a reduced interface area (470.7 Å^2) and a slightly more favorable binding free energy (−1.5 kcal/mol), indicating that ultrasound treatment alters the binding interface but does not significantly enhance the interaction. In contrast, the ultrasonication-treated OVA with trypsin complex exhibited a larger interface area (857.9 Å^2) and a significantly more favorable binding free energy (−5.0 kcal/mol), suggesting that ultrasound treatment enhances the binding affinity between OVA and trypsin.

Table 1
Protein-protein interaction parameters for OVA complexes with pepsin and trypsin under native and ultrasound-treated conditions.

Complex	Interface area (Å^2)	ΔG (kcal/mol)	P-value
Native OVA-Pepsin	998.4	−0.9	0.736
Native OVA-Trypsin	773.3	−3.8	0.449
OVA-US-Pepsin	470.7	−1.5	0.512
OVA-US-Trypsin	857.9	−5.0	0.376

To further elucidate the binding interactions between OVA (Chain A) and the digestive enzymes pepsin and trypsin (Chain B), LigPlot analysis was conducted to visualize hydrogen bonding and hydrophobic interactions at the interface, as shown in Fig. 5B-C. In the case of ultrasound-treated OVA with pepsin digestion, hydrogen bonds were primarily formed between residues such as Arg199 (B) and Ser296 (A), while hydrophobic interactions involved residues including Gln163 (A),

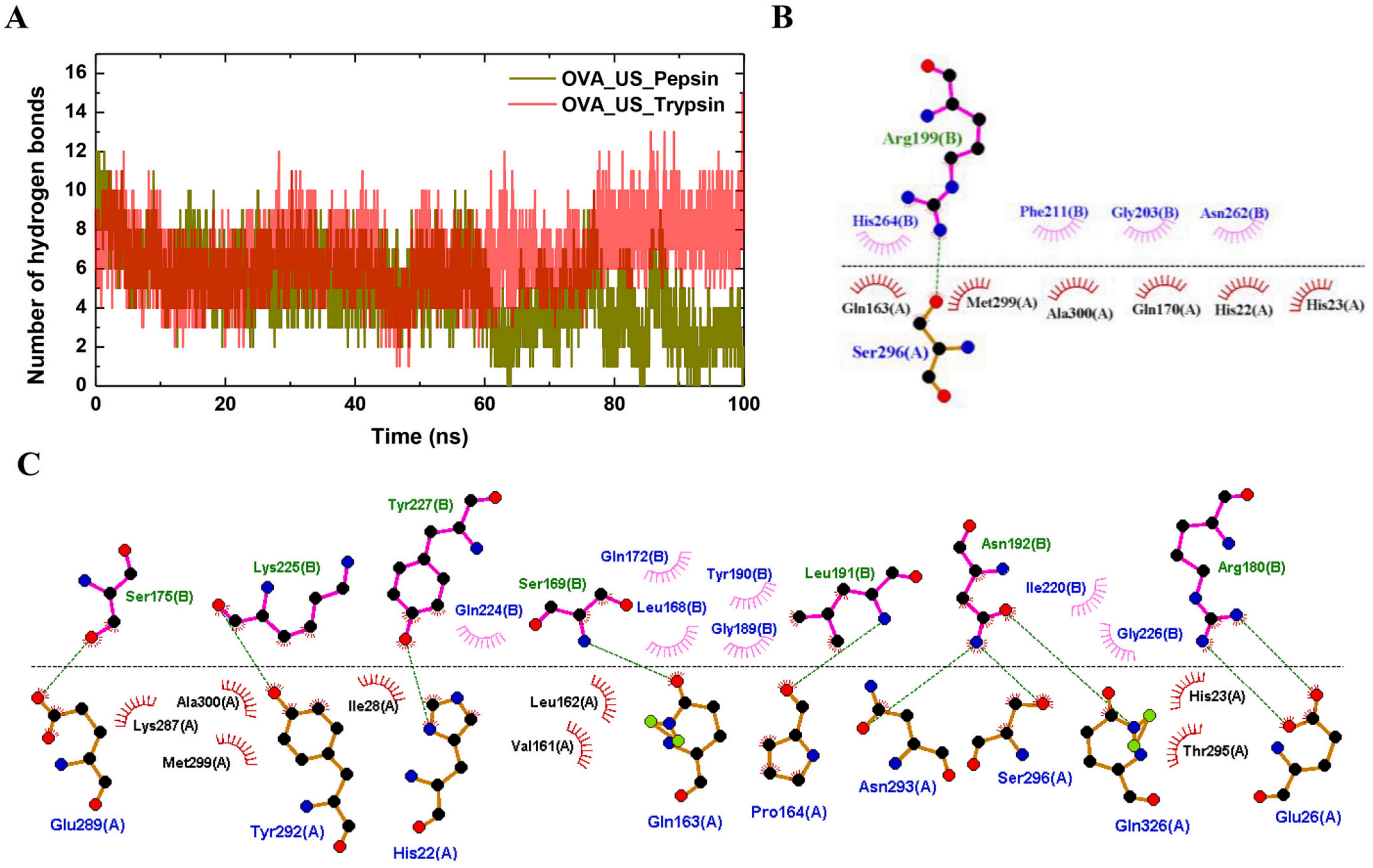

Fig. 5. Interaction diagram of the OVA with pepsin and trypsin. (A) Number of hydrogen bonds formed between OVA and the enzymes pepsin and trypsin over the 100 ns molecular dynamics simulation. The plot illustrates the dynamic changes in hydrogen bond interactions. LigPlot representation of the OVA-Pepsin complex (B) and OVA-Trypsin complex (C, highlighting hydrogen bonds (green dashed lines) and hydrophobic interactions (red arcs). Chain A represents OVA and chain B represents enzyme. (For interpretation of the references to colour in this figure legend, the reader is referred to the web version of this article.)

His22 (A), and Met299 (A). This interaction profile correlates with the relatively weak binding affinity observed in the PISA analysis.

4. Discussion

Ultrasound treatment can promote the enzymatic hydrolysis of proteins (Jian Jin et al., 2016; S. Li et al., 2016). Our study found that ultrasound treatment potentially enhances its gastrointestinal digestion, suggesting that ultrasound treatment may facilitate conformational changes, degradation of allergenic epitopes in OVA, thereby reducing its allergenicity. Similar findings were observed which shows that a significant reduction in α-helix content of egg white is significantly reduced by 400 W ultrasound for 16 min, compared to untreated samples (Zhu et al., 2018a). Ultrasound treatment can disrupt protein interactions, potentially reducing the allergenicity of the protein by promoting the unfolding of the secondary structure. Previous study also found that the α-helix content of OVA significantly decreases after digestion (Martos et al., 2010). Fluorescence spectroscopy reflects the exposure level of aromatic tryptophan residues in OVA. After *in vitro* digestion of chicken protein, the intrinsic fluorescence intensity significantly decreases, indicating the disruption of the protein's tertiary structure (Bai et al., 2023). In a study on *in vitro* digestion of ultrasound-treated buckwheat protein, the surface hydrophobicity and free sulfhydryl content of buckwheat protein increased (J. Jin et al., 2021). The results of this study show that the intrinsic fluorescence intensity of OVA significantly decreased after gastrointestinal digestion. This may be due to the digestive enzymes breaking the disulfide bonds, leading to the unfolding of the OVA structure and the subsequent exposure of tryptophan residues, whose fluorescence is quenched by the environment. It is also reported that ultrasonic treatment induces conformational changes and alterations in the physicochemical properties of shrimp myosin, leading to the exposure of cleavage sites for pepsin and trypsin, and subsequently enhanced digestibility and reduced allergenicity (Zhang et al., 2018a). The ultrasound-induced conformational epitopes and physicochemical changes in OVA may have facilitated its interaction with digestive enzymes, hereby reducing allergenicity.

The allergenicity of proteins is related to the integrity of allergenic epitopes, which consist of linear and conformational epitopes, and can be recognized by specific antibodies (Zhou et al., 2016). IgE binding capacity of Act d 2 is significantly inhibited after ultrasound processing (J. Wang et al., 2021). High intensity ultrasound enhances the IgG and IgE binding of OVA (W. H. Yang et al., 2017). The different results might be resulted from the difference in molecular weight, stability of conformational structures, the exposure of IgE epitopes, as well as the different processing temperature during ultrasound treatment (Rahaman et al., 2016). Although our study primarily focused on the combined effects of ultrasound and enzymatic digestion, preliminary ELISA data (not shown) indicated that ultrasound treatment alone also reduced IgE-binding capacity to a certain extent. However, the residual IgE reactivity observed suggests that ultrasound alone may not be sufficient to eliminate allergenicity. Therefore, enzymatic digestion remains essential for further reducing allergenic potential. Ultrasound treatment induced conformational changes in shrimp myosin, leading to the exposure of cleavage sites for pepsin and trypsin, thereby enhancing digestibility and reducing allergenicity (Zhang et al., 2018b). After *in vitro* digestion, the IgG and IgE binding capacities of allergenic proteins from almonds, pine nuts, and peanuts were significantly reduced. Following gastrointestinal digestion of peanut proteins, Ara h 1 and Ara h 3 were partially hydrolyzed, and their IgE binding capacity was significantly decreased (Toomer et al., 2013). Similarly, the IgE binding capacity of hydrolyzed peptides from OVM significantly decreased after gastric digestion (Takagi et al., 2005).

The allergenicity of OVA was evaluated using both polyclonal IgE from sera of OVA-sensitized mice and a commercially available monoclonal anti-OVA IgE antibody. While these immunoassays are widely accepted for preclinical allergenicity assessment, it is important to note that murine IgE profiles may not fully replicate the complexity and specificity of human allergic responses. Allergenicity is highly individual and species-dependent, as IgE epitopes recognized in animal models may differ from those relevant in humans due to variations in immune recognition patterns (Dearman & Kimber, 2009). Nevertheless, murine models provide valuable mechanistic insights into allergen structure-immunoreactivity relationships and are extensively used in food allergy research to evaluate processing-induced changes (Benedé & Berin, 2020). This study found that the allergenicity of OVA *in vitro* digestion products decreased with increasing ultrasound treatment time, suggesting that the epitopes of OVA may be disrupted. To enhance translational relevance, future studies should incorporate human allergic sera to validate whether ultrasound-induced modifications in OVA structure effectively reduce IgE reactivity in clinically sensitized individuals.

OVA was very resistant to pepsin action, immunoreactivity of OVA against IgE from sera of allergic patients was retained after *in vitro* gastric digestion, but it decreased considerably after *in vitro* duodenal digestion (Martos et al., 2010). Under ultrasound treatment, the OVA-Pepsin complex displayed a disruption in hydrophobic interactions and hydrogen bond interactions involving residues such as His22 (A), Ala24 (A), Glu26 (A), Phe307 (A), Ser308 (A), Lys323 (A), and Ser325 (A), as we reported the interactions in our previous study for native OVA-Pepsin complex (J. Yang et al., 2025). In contrast, the OVA-Trypsin complex exhibited a broader array of stabilizing interactions under ultrasonic treatment. Key hydrogen bonds involved residues such as His22 (A), Glu26 (A), Gln163 (A), Pro164 (A), Glu289 (A), Tyr292 (A), Asn293 (A), Ser296 (A), and Gln326 (A), along with extensive hydrophobic contacts. These interactions contribute to the stronger binding affinity of trypsin for OVA. Under ultrasonic conditions, residues such as Glu26 (A), Glu289 (A), and Ser296 (A) remained involved in forming hydrogen bonds, along with a new set of residues compared to the native OVA-Trypsin complex (J. Yang et al., 2025). The enhanced hydrogen bond and hydrophobic interactions contributed to the improved binding affinity observed in the PISA analysis. Some common sequences of the OVA linear IgE epitopes, such as 159–172, 323–332, 95–102 (Behzad Gazme et al., 2022), which are involved in these hydrogen bond interactions. These results indicate that enzymatic cleavage of epitope-containing regions may modify IgE-binding sites in OVA, consequently attenuating its allergenicity. This observation is consistent with prior research demonstrating that pepsin and trypsin digestion can degrade allergenic epitopes (Foster et al., 2013; Hu et al., 2021), thereby diminishing OVA's immunogenic potential. Although computational simulations (docking and MD) offer important structural and dynamic insights, additional *in vivo* validation is required to confirm whether the ultrasound-mediated reduction in allergenicity effectively decreases IgE reactivity under physiological conditions. Notably, residue-wise fluctuations were pronounced in epitope-rich regions such as 77–84, 95–102, 188–198, 347–385, which have been identified as major linear IgE-binding epitopes in OVA (Behzad Gazme et al., 2022; Li et al., 2022b). This localized flexibility suggests that ultrasound facilitates structural destabilization of epitopes, increasing their accessibility to enzymatic cleavage and consequently reducing their immunogenic potential. These MD-derived conformational changes correlate strongly with the experimentally observed reduction in IgE-binding (Fig. 1C-D), decrease in α-helix content and increase in β-sheet structures (Fig. 2B), and enhanced surface hydrophobicity (Fig. 2F), all of which reflect protein unfolding and epitope exposure (J. Jin et al., 2021; Zhou et al., 2016). Moreover, the LigPlot and PISA interaction analyses (Fig. 5B-C, Table 1) revealed strengthened hydrogen bonding and hydrophobic interactions between OVA and trypsin under ultrasonic treatment, aligning with increased enzymatic susceptibility and epitope degradation. These results are consistent with prior reports that epitope flexibility and solvent exposure play crucial roles in IgE recognition and allergenic potential (Foster et al., 2013).

Despite the valuable insights provided by this study, several limitations should be acknowledged. First, the *in vitro* digestion model,

although widely used and standardized (Abraham et al., 2015), cannot fully replicate the dynamic and complex physiological conditions of the human gastrointestinal tract, such as peristalsis, mucus secretion, or interactions with gut microbiota. Second, the evaluation of IgE-binding capacity using murine polyclonal sera and monoclonal antibodies, while informative for mechanistic understanding, may not fully reflect human allergenic responses due to species-specific differences in immune recognition (Dearman & Kimber, 2009). Third, clinical validation using sera from egg-allergic individuals or *in vivo* models was not included, which limits the direct translational applicability of the findings. Therefore, future studies should incorporate human allergic patient sera for ELISA testing and consider clinical trials or humanized animal models to confirm the allergenicity-reducing effects of ultrasound treatment. Additionally, integrating immunoblotting or basophil activation assays may offer a more comprehensive evaluation of immunogenic potential.

5. Conclusion

This work described the structure and allergenicity changes of ultrasound treated-OVA observed under *in vitro* digestion. Applying ultrasound (60 min) accelerated enzymatic hydrolysis of OVA, led to the alterations in the microstructure and unfolding of the molecular structure in OVA during *in vitro* digestion. These results collectively demonstrate that ultrasound treatment significantly influences the binding interactions between OVA and the enzymes, particularly enhancing the interaction with trypsin. The stronger binding affinity and larger interface area observed for the ultrasonication-treated OVA with trypsin are consistent with the structural changes observed in the RMSD, Rg, and RMSF analyses, further supporting the hypothesis that ultrasound and trypsin digestion synergistically disrupt native structure of OVA. These findings confirm that epitope residues are associated with the enzyme interactions with the ultrasonication-treated OVA, which could potentially impact OVA allergenicity.

CRediT authorship contribution statement

Jing Yang: Writing – review & editing, Supervision, Project administration, Funding acquisition. **Nandan Kumar:** Writing – original draft, Software, Investigation. **Hong Kuang:** Writing – original draft, Methodology, Investigation, Formal analysis, Data curation. **Yonghui Li:** Writing – review & editing, Supervision, Conceptualization. **Jiajia Song:** Writing – review & editing.

Declaration of competing interest

The authors assert that they do not have any competing financial interests that could be perceived to influence the work reported in this paper.

Acknowledgements

This study was supported by Natural Science Foundation of Chongqing (Grant No. cstc2021jcyj-msxmX0712; CSTB2024NSCQ-MSX0745).

Appendix A. Supplementary data

Supplementary data to this article can be found online at https://doi.org/10.1016/j.foodchem.2025.146015.

Data availability

The data that has been used is confidential.

References

Abraham, M. J., Murtola, T., Schulz, R., Páll, S., Smith, J. C., Hess, B., & Lindahl, E. (2015). GROMACS: High performance molecular simulations through multi-level parallelism from laptops to supercomputers. *SoftwareX, 1*, 19–25.
Bai, X., Shi, S., Kong, B., Chen, Q., Liu, Q., Li, Z., Wu, K., & Xia, X. (2023). Analysis of the influencing mechanism of the freeze–thawing cycles on in vitro chicken meat digestion based on protein structural changes. *Food Chemistry, 399*, Article 134020.
Benedé, S., & Berin, M. C. (2020). Applications of mouse models to the study of food allergy. *Animal Models of Allergic Disease: Methods and Protocols*, 1–17.
Brodkorb, A., Egger, L., Alminger, M., Alvito, P., Assunção, R., Ballance, S., Bohn, T., Bourlieu-Lacanal, C., Boutrou, R., & Carrière, F. (2019). INFOGEST static *in vitro* simulation of gastrointestinal food digestion. *Nature Protocols, 14*(4), 991–1014.
Bu, G., Luo, Y., Chen, F., Liu, K., & Zhu, T. (2013). Milk processing as a tool to reduce cow's milk allergenicity: A mini-review. *Dairy Science & Technology, 93*(3), 211–223.
Dearman, R., & Kimber, I. (2009). Animal models of protein allergenicity: Potential benefits, pitfalls and challenges. *Clinical & Experimental Allergy, 39*(4), 458–468.
Foster, E. S., Kimber, I., & Dearman, R. J. (2013). Relationship between protein digestibility and allergenicity: Comparisons of pepsin and cathepsin. *Toxicology, 309*, 30–38.
Gao, Q., Yang, Y.-Q., Nie, H.-N., Wang, B.-Q., Peng, X., Wang, N., Li, J.-K., Rao, J.-J., & Xue, Y.-L. (2024). Investigating the impact of ultrasound on the structural, physicochemical, and emulsifying characteristics of Dioscorin: Insights from experimental data and molecular dynamics simulation. *Food Chemistry, 453*, Article 139581.
Gazme, B., Rezaei, K., & Udenigwe, C. C. (2020). Effect of enzyme immobilization and in vitro digestion on the immune-reactivity and sequence of IgE epitopes in egg white proteins. *Food & Function, 11*(7), 6632–6642.
Gazme, B., Rezaei, K., & Udenigwe, C. C. (2022). Epitope mapping and the effects of various factors on the immunoreactivity of main allergens in egg white. *Food & Function, 13*(1), 38–51.
Han, Y., Wang, N., Guo, X., Jiao, T., & Ding, H. (2022). Influence of ultrasound on the adsorption of single-walled carbon nanotubes to phenol: A study by molecular dynamics simulation and experiment. *Chemical Engineering Journal, 427*, Article 131819.
Hu, J., Yuan, L., An, G., Zhang, J., Zhao, X., Liu, Y., Shan, J., & Wang, Z. (2021). Antigenic activity and epitope analysis of β-conglycinin hydrolyzed by pepsin. *Journal of the Science of Food and Agriculture, 101*(4), 1396–1402.
Jin, J., Ma, H., Wang, W., Luo, M., Wang, B., Qu, W., He, R., Owusu, J., & Li, Y. (2016). Effects and mechanism of ultrasound pretreatment on rapeseed protein enzymolysis. *Journal of the Science of Food and Agriculture, 96*(4), 1159–1166.
Jin, J., Okagu, O. D., Yagoub, A. E. A., & Udenigwe, C. C. (2021). Effects of sonication on the in vitro digestibility and structural properties of buckwheat protein isolates. *Ultrasonics Sonochemistry, 70*, Article 105348.
Laskowski, R. A., Jabłońska, J., Pravda, L., Vařeková, R. S., & Thornton, J. M. (2018). PDBsum: Structural summaries of PDB entries. *Protein Science, 27*(1), 129–134.
Li Li, M., Tan, W., Liu, X., & Duan, X. (2019). Effects of ball-milling treatment on physicochemical and foaming activities of egg ovalbumin. *Journal of Food Engineering, 261*, 158–164.
Li, S., Yang, X., Zhang, Y., Ma, H., Liang, Q., Qu, W., … Mahunu, G. K. (2016). Effects of ultrasound and ultrasound assisted alkaline pretreatments on the enzymolysis and structural characteristics of rice protein. *Ultrasonics Sonochemistry, 31*, 20–28.
Li, Y., Zhang, S., Ding, J., Zhong, L., Sun, N., & Lin, S. (2022a). Evaluation of the structure-activity relationship between allergenicity and spatial conformation of ovalbumin treated by pulsed electric field. *Food Chemistry, 388*(15), Article 133018.
Li, Y., Zhang, S., Ding, J., Zhong, L., Sun, N., & Lin, S. (2022b). Evaluation of the structure-activity relationship between allergenicity and spatial conformation of ovalbumin treated by pulsed electric field. *Food Chemistry, 388*, Article 133018.
Liu, W. L., Wang, H., Hu, Y. M., Wang, X. M., Chen, H. Q., & Tu, Z. C. (2023). Mechanism of the allergenicity reduction of ovalbumin by microwave pretreatment-assisted enzymolysis through biological mass spectrometry. *Journal of Agricultural and Food Chemistry, 71*(41), 15363–15374.
López-Expósito, I., Chicón, R., Belloque, J., Recio, I., Alonso, E., & López-Fandiño, R. (2008). Changes in the ovalbumin proteolysis profile by high pressure and its effect on IgG and IgE binding. *Journal of Agricultural and Food Chemistry, 56*(24), 11809–11816.
Mack, D. P., Greenhawt, M., & Anagnostou, A. (2023). Are there hidden dangers associated with milk and egg dietary advancement therapy? *The journal of allergy and clinical immunology: In Practice, 11*(4), 1056–1062.
Martos, G., Contreras, P., Molina, E., & Lopez-Fandino, R. (2010). Egg white ovalbumin digestion mimicking physiological conditions. *Journal of Agricultural and Food Chemistry, 58*(9), 5640–5648.
Rahaman, T., Vasiljevic, T., & Ramchandran, L. (2016). Effect of processing on conformational changes of food proteins related to allergenicity. *Trends in Food Science & Technology, 49*, 24–34.
Takagi, K., Teshima, R., Okunuki, H., Itoh, S., Kawasaki, N., Kawanishi, T., Hayakawa, T., Kohno, Y., Urisu, A., & Sawada, J. (2005). Kinetic analysis of pepsin digestion of chicken egg white ovomucoid and allergenic potential of pepsin fragments. *International Archives of Allergy and Immunology, 136*(1), 23–32.
Taniguchi, H., Ogura, K., Sato, S., Ebisawa, M., & Yanagida, N. (2022). Natural history of allergy to hen's egg: A prospective study in children aged 6 to 12 years. *International Archives of Allergy and Immunology, 183*(1), 14–24.
Tao, Y., & Sun, D.-W. (2015). Enhancement of food processes by ultrasound: A review. *Critical Reviews in Food Science and Nutrition, 55*(4), 570–594.
Toomer, O. T., Do, A., Pereira, M., & Williams, K. (2013). Effect of simulated gastric and intestinal digestion on temporal stability and immunoreactivity of peanut, almond,

and pine nut protein allergens. *Journal of Agricultural and Food Chemistry, 61*(24), 5903–5913.
Wallace, A. C., Laskowski, R. A., & Thornton, J. M. (1995). LIGPLOT: A program to generate schematic diagrams of protein-ligand interactions. *Protein Engineering, Design and Selection, 8*(2), 127–134.
Wang, C., Xie, Q., Wang, Y., & Fu, L. (2020). Effect of ultrasound treatment on allergenicity reduction of milk casein via colloid formation. *Journal of Agricultural and Food Chemistry, 68*(16), 4678–4686.
Wang, J., Wang, J., Vanga, S. K., & Raghavan, V. (2021). Influence of high-intensity ultrasound on the IgE binding capacity of act d 2 allergen, secondary structure, and in-vitro digestibility of kiwifruit proteins. *Ultrasonics Sonochemistry, 71*, Article 105409.
Xiong, W., Wang, Y., Zhang, C., Wan, J., Shah, B. R., Pei, Y., … Li, B. (2016). High intensity ultrasound modified ovalbumin: Structure, interface and gelation properties. *Ultrasonics Sonochemistry, 31*, 302–309.
Yang, J., Kuang, H., Kumar, N., Song, J., & Li, Y. (2024). Changes of structure properties and potential allergenicity of ovalbumin under high hydrostatic pressures. *Food Research International, 190*, Article 114658.
Yang, J., Kumar, N., Kuang, H., Song, J., & Li, Y. (2025). Changes of digestive stability and potential allergenicity of high hydrostatic pressure-treated ovalbumin during in vitro digestion. *Food Chemistry, 142962*.
Yang, W. H., Tu, Z. C., Wang, H., Li, X., & Tian, M. (2017). High-intensity ultrasound enhances the immunoglobulin (Ig)G and IgE binding of ovalbumin. *Journal of the Science of Food and Agriculture, 97*(9), 2714–2720.
Zhang, Z., Zhang, X., Chen, W., & Zhou, P. (2018a). Conformation stability, in vitro digestibility and allergenicity of tropomyosin from shrimp (Exopalaemon modestus) as affected by high intensity ultrasound. *Food Chemistry, 245*, 997–1009.
Zhang, Z., Zhang, X., Chen, W., & Zhou, P. (2018b). Conformation stability, in vitro digestibility and allergenicity of tropomyosin from shrimp (Exopalaemon modestus) as affected by high intensity ultrasound. *Food Chemistry, 245*, 997–1009.
Zhou, H., Wang, C., Ye, J., Chen, H., Tao, R., & Cao, F. (2016). Effects of high hydrostatic pressure treatment on structural, allergenicity, and functional properties of proteins from ginkgo seeds. *Innovative Food Science & Emerging Technologies, 34*, 187–195.
Zhu, Y., Vanga, S. K., Wang, J., & Raghavan, V. (2018a). Effects of ultrasonic and microwave processing on avidin assay and secondary structures of egg white protein. *Food and Bioprocess Technology, 11*, 1974–1984.
Zhu, Y., Vanga, S. K., Wang, J., & Raghavan, V. (2018b). Impact of food processing on the structural and allergenic properties of egg white. *Trends in Food Science & Technology, 78*, 188–196.